Percolation description of charge transport in amorphous oxide semiconductors

A. V. Nenashev,[1,2] J. O. Oelerich,[3] S. H. M. Greiner,[3] A. V. Dvurechenskii,[1,2] F. Gebhard,[3] and S. D. Baranovskii[3,*]

[1]*Institute of Semiconductor Physics, 630090 Novosibirsk, Russia*

[2]*Novosibirsk State University, 630090 Novosibirsk, Russia*

[3]*Department of Physics and Material Sciences Center, Philipps-University, D-35032 Marburg, Germany*

(Received 11 July 2019; revised manuscript received 20 August 2019; published 12 September 2019)

The charge transport mechanism in amorphous oxide semiconductors (AOS) is a matter of controversial debates. Most theoretical studies so far neglected the percolation nature of the phenomenon. In this paper, a recipe for theoretical description of charge transport in AOSs is formulated using the percolation arguments. Comparison with the previous theoretical studies shows a superiority of the percolation approach. The results of the percolation theory are compared to experimental data obtained in various InGaZnO materials revealing parameters of the disorder potential in such AOS.

DOI: 10.1103/PhysRevB.100.125202

I. INTRODUCTION

Amorphous oxide semiconductors such as InGaZnO (IGZO) systems are in the focus of intensive research due to applications of these materials in thin-film transistors for transparent and flexible flat-panel displays. Although charge transport plays a decisive role for such applications, there is no agreement on the basic transport mechanism. In particular, the percolation nature of charge transport inherent for electrical conduction in disordered materials has not been addressed properly thus far. In the present work, we develop a concise description of charge transport in AOS based on the percolation theory.

In solids, there are basically three distinct transport mechanisms, and all of them were suggested as possible candidates for charge transport in AOS. In the following, we discuss them briefly before we describe the random band-edge model that looks most plausible for amorphous oxide semiconductors.

A. Band transport via extended states in the random barrier model

In their pioneering works [1–5], Hosono and collaborators proposed band transport via extended states as a possible transport mechanism in IGZO materials. They assumed that charge carriers can move above the band edge E_m but their motion is affected by a disorder in the form of random potential barriers with a Gaussian distribution of heights,

$$G_B(V) = \frac{1}{\delta_\phi\sqrt{2\pi}} \exp\left(-\frac{(V-\phi_0)^2}{2{\delta_\phi}^2}\right). \tag{1}$$

Here, ϕ_0 is the average height of the barriers and δ_ϕ is the standard deviation in the distribution of the barrier heights. This random barrier model is sketched in Fig. 1.

Charge transport in the random barrier model was described in the framework of the Drude approach that is based on the average relaxation time $\langle\tau\rangle$ for free carriers in the states above the band edge E_m. In this approximation, the carrier mobility is determined as $\mu = e\langle\tau\rangle/m$, where m is the effective mass. For the band transport in the absence of a disorder potential, the Drude approach leads to the expression [4,6–8]

$$\mu = -\frac{e}{m\cdot n}\int_{E_m}^{\infty}\tau(E)v_z(E)\frac{\partial f_e(E)}{\partial v_z}D_m(E)dE\ , \tag{2}$$

where n is the concentration of carriers, $\tau(E)$ is the momentum relaxation time at the electron energy E, $v_z(E)$ is the electron velocity along the transport direction (z axis), $D_m(E)$ is the density of states above the band edge E_m, and $f_e(E)$ is the Fermi function.

In the presence of substantial disorder in AOS, the Drude approach is then modified heuristically by the introduction of the weight function [4]

$$\varrho(E) = \int_E^{\infty} G_B(\varepsilon)d\varepsilon\ , \tag{3}$$

which was termed "transmission probability" [4]. The expression for the charge carrier mobility in AOS thus attains the form

$$\mu = -\frac{e}{m\cdot n}\int_{E_m}^{\infty}\tau(E)v_z(E)\varrho(E)\frac{\partial f_e(E)}{\partial v_z}D_m(E)dE\ . \tag{4}$$

The introduction of the weight function $\varrho(E)$ into Eq. (4) was interpreted [4] as taking into account the percolation arguments suggested by Adler *et al.* [9]. However, percolation has little to do with Eqs. (3) and (4), as is readily seen from the fact that the percolation threshold does not appear in the above equations. This feature will be discussed in Sec. III.

More importantly, if disorder creates potential barriers above the band edge as sketched in Fig. 1, it will also create potential wells below the band edge. The statistical distribution of these wells must be taken into account as well, which makes E_m a regional, random quantity (random band-edge model). A description of charge transport based on percolation theory for the random band-edge model will be given in Sec. III.

*baranovs@staff.uni-marburg.de

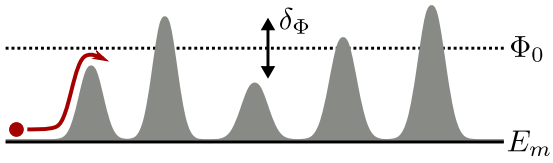

FIG. 1. Random barrier model for band transport above the band edge E_m affected by random potential barriers.

B. Trap-limited band transport

Trap-limited transport in the spirit of the multiple-trapping (MT) model has also been considered as a possible transport mechanism in AOS [10,11]. In the MT process, the motion of charge carriers via delocalized states is interrupted by trapping into the localized states with subsequent activation of carriers back into the conducting states above the mobility edge.

The energy spectrum of localized states in the band tails of inorganic amorphous semiconductors is widely considered to exhibit a purely exponential shape [12–16],

$$g(E) = N_m \exp\left(\frac{E}{E_0}\right), \tag{5}$$

where E is the energy of the trap counted from the band edge E_m, E_0 is the energy scale, and N_m is the density of localized states at the band edge E_m. Lee *et al.* [11] used an extraction technique to determine the subgap density of states in an n-channel amorphous InGaZnO (a-IGZO) thin-film transistor based on the study of the multifrequency capacitance-voltage (C–V) characteristics. They concluded that the subgap density of states is a superposition of two distinct coexisting exponential functions. Lee *et al.* [17,18] combined the above models of band transport limited by potential barriers [1,3–5] and the multiple-trapping transport [10,11]. Consequently, they assume two distinct transport regimes in a thin-film transistor based on AOS, depending on the concentration of carrier. At low gate voltages, i.e., at small carrier concentrations n, the Fermi level lies in the manifold of the localized states, characterized by the density of states given by Eq. (5), with energies below the band edge E_m. In this MT regime, the drift mobility of carriers is determined as

$$\mu \simeq \mu_{\rm mod} \frac{n_{\rm free}}{n_{\rm free} + n_{\rm trap}}, \tag{6}$$

where $n_{\rm free}$ and $n_{\rm trap}$ are the free (above E_m) and trapped (below E_m) carrier densities, respectively, and $\mu_{\rm mod}$ is treated as the usual band mobility μ_0, "modulated by the percolation term" [17]. Lee *et al.* [17] mention that this term should be determined by the ratio between the potential barrier height and the average barrier width. Nevertheless, they use the relation between $\mu_{\rm mod}$ and μ_0, derived by the averaging of transition rates for overcoming potential barriers. The latter method has been, however, qualified as not appropriate for description of incoherent charge transport [15,19].

C. Hopping transport

The incoherent tunneling of charge carriers between localized states, distributed randomly in space and energy, also has been suggested as a possible charge transport mechanism in IGZO materials [8]. A marginal admixture of band transport was also assumed in order to account for the Hall measurements. The theoretical analysis by Germs *et al.* [8] is based on the concept of the transport energy E_t. According to this approach, charge transport in a system with localized electron states is due to the activation of carriers from the Fermi level E_f towards the vicinity of the transport energy [20–24]. The carrier mobility in this transport regime can be written as [15,25–27]

$$\mu = \widetilde{\mu_0} \exp\left[-\frac{E_t - E_f(n,T)}{kT}\right], \tag{7}$$

where E_t is the transport energy and the prefactor $\widetilde{\mu_0}$ depends on the concentration of carriers n.

At very low temperatures, this equation should be replaced by Mott or Efros-Shklovskii approach to the variable-range hopping (VRH) [12,19]. The quantitative criteria on temperature for the exponential distribution of localized states [8] were discussed elsewhere [28]. In Ref. [4], experimental data in c-IGZO were fitted using the Mott approach to VRH, though the VRH regime was rejected due to arguments based on Hall measurements [4].

To fit with Eq. (7) the high values of the carrier mobility measured in IGZO materials, an unusually large value of the localization length in the tail states, $a \simeq 4.8$ nm, is needed in the model of hopping transport [8]. This value exceeds by far the estimates for the localization length of carriers in the band tails of inorganic semiconductors [12–15]. Therefore, it appears unlikely that hopping transport is the dominant mechanism for charge transport in AOS.

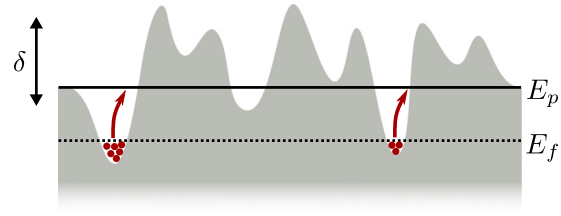

FIG. 2. Schematic representation of the spatial fluctuations of the band edge E_m in the random band-edge model. The carrier motion is due to activation from the Fermi level E_f towards the percolation level E_p.

D. Random band-edge model

Recently, Fishchuk *et al.* [29] addressed a model that combines band transport and localized band-tail states, though with a significant modification. While Kamiya *et al.* [2,4] and Lee *et al.* [17,18] assume the distribution of potential barriers of the form given by Eq. (1) above a global band edge E_m, see Fig. 1, Fishchuk *et al.* [29] assume that the disorder potential causes random long-range variations of the band edge E_m, as illustrated in Fig. 2. The spatial fluctuations of the band edge E_m are assumed to be Gaussian with the distribution function [29]

$$G(E_m) = \frac{1}{\delta\sqrt{2\pi}} \exp\left[-\frac{1}{2}\left(\frac{E_m}{\delta}\right)^2\right], \tag{8}$$

where δ is the standard deviation, and the position of the band edge E_m is counted from the position of the band edge without

disorder potential. In this work, we consider the random band-edge model suggested by Fishchuk *et al.* [29] as appropriate for the description of charge transport in AOS.

Fishchuk *et al.* [29] applied the effective-medium-approximation (EMA) to a theoretical study of charge transport. In contrast, we use percolation arguments to develop a theoretical description of charge transport in the random band-edge model. At $kT \ll \delta$, where kT is the thermal energy and δ is the scale of disorder in Eq. (8), the results of our percolation theory are reliable and they substantially differ from those of the EMA approach used previously [29], as shown in Sec. IV. Therefore, the percolation theory seems superior to the EMA for the description of charge transport within the random band-edge model.

E. Outline

In Sec. II, we describe in more detail the random band-edge model of Fishchuk *et al.* [29] that we employ for our study. In Sec. III, we show how to calculate the carrier mobility using percolation theory. In Sec. IV, we compare our percolation approach with the effective medium approximation. In Sec. V, we compare our theoretical results with experimental data. It is shown that percolation theory is capable of accounting for the dependencies of the charge carrier mobility on temperature and on the concentration of charge carriers in IGZO materials. Moreover, a comparison between the results of percolation theory with experimental data reveals the characteristic parameter δ of the band-edge disorder in Eq. (8) and the conduction-electron mobility μ_0.

II. RANDOM BAND-EDGE MODEL FOR CHARGE TRANSPORT IN AOS

The random band-edge model by Fishchuk *et al.* [29] assumes that the position of the band edge E_m varies in space due to disorder potential. The distribution of E_m values that belong to different spatial regions is characterized by the Gaussian distribution $G(E_m)$ given by Eq. (8). This distribution in the regional positions of the band edge plays a crucial role in the rest of this paper.

For the sake of completeness, we also include localized states with energies below E_m, whose density of states is assumed to be exponential, see Eq. (5), where the energy E is counted from the band edge E_m. Following Fishchuk *et al.* [29], we assume that the delocalized states with energies above E_m are characterized by the density of states

$$g(E - E_m) = g_c \sqrt{E - E_m + \Delta E}\ , \tag{9}$$

where the value $g_c = 1.4 \times 10^{21}\ \mathrm{cm}^{-3}\,\mathrm{eV}^{-3/2}$ has been reported for a-IGZO thin films [4]. Equations (9) and (5) can be combined to the *regional* density of states

$$g(E - E_m) = \Theta(E - E_m)\, g_c \sqrt{E - E_m + (N_m/g_c)^2} + \left[1 - \Theta(E - E_m)\right] N_m \exp\left(\frac{E - E_m}{E_0}\right), \tag{10}$$

where $\Theta(x)$ is the Heaviside step function. The first term on the right-hand side describes the density of delocalized states above E_m, and the second term describes the density of localized states below E_m. The energy shift ΔE in Eq. (9) guarantees the continuity of the density of states at $E = E_m$ when we choose $\Delta E = (N_m/g_c)^2$.

For a given value of E_m, one can find a corresponding *regional* electron density,

$$n_{\mathrm{region}}(E_m) = \int_{-\infty}^{+\infty} g(E - E_m)\, f(E)\, dE\ , \tag{11}$$

where $f(E)$ is the Fermi function,

$$f(E) = \left[\exp\left(\frac{E - E_f}{kT}\right) + 1\right]^{-1}\ , \tag{12}$$

and E_f is the Fermi level. The *total* electron density n, averaged over the regional positions of the mobility edge E_m, is

$$n = \int_{-\infty}^{+\infty} G(E_m)\, n_{\mathrm{region}}(E_m)\, dE_m\ . \tag{13}$$

For given temperature T and electron concentration n, the position of the Fermi level E_f can be found from the system of Eqs. (10)–(13).

The AOS material is assumed to be a medium with a smoothly varying regional conductivity σ_{region}, which is a product of the elementary charge e, the conduction-band electron mobility μ_0, and the local concentration of mobile electrons (with energies above E_m),

$$\sigma_{\mathrm{region}}(E_m) = e\mu_0 \int_{E_m}^{+\infty} g(E - E_m)\, f(E)\, dE\ . \tag{14}$$

This assumption is justified when the electron mean-free path is small compared to the spatial scale for variations of E_m. Coefficient μ_0 is the intrinsic (band) charge-carrier mobility in extended states determined by the electron effective mass and the average scattering time. It may depend on temperature and also on the electron concentration in the case of a degenerate system. However, one cannot study the dependence of μ_0 on T and n without deep understanding of the electron scattering mechanisms in the given material. Therefore, following Fishchuk *et al.* [29] we consider μ_0 as a constant for the sake of simplicity. Below we will focus on the exponential factor in the temperature dependence of the drift mobility leaving the pre-exponential factor containing μ_0 as a fitting parameter.

The global (macroscopic) conductivity σ is to be found by some "averaging" of the regional values $\sigma_{\mathrm{region}}(E_m)$, taking into account the Gaussian distribution $G(E_m)$ of the mobility edge E_m, i.e., $\sigma = \langle \sigma_{\mathrm{region}} \rangle$. When the global σ is found, one can calculate the (measured) mobility μ as

$$\mu = \frac{\sigma}{en}\ . \tag{15}$$

In the case of an exponentially broad scatter of regional conductivities, a proper choice of the averaging procedure is crucial for a correct determination of the global conductivity σ. We will consider three methods of "averaging": The first is based on the effective medium approximation, expressed by Eq. (31), see Sec. IV; the other two procedures are based on percolation theory expressed by Eqs. (19) and (25), see Sec. III.

For the experimentally accessible regions of the (n, T) phase diagram of IGZO materials, Fishchuk *et al.* [29] have shown that the conductivity $\sigma(n, T)$ and the mobility $\mu(n, T)$ depend on the carrier concentration n and the temperature T mostly through the variations of the conduction-band edge E_m, and are not limited by the localized states. Therefore, localized states might be disregarded in IGZO films.

III. PERCOLATION THEORY FOR CHARGE TRANSPORT IN THE RANDOM BAND-EDGE MODEL

A. From regional to global conductivities in continuum percolation theory

The random band-edge model belongs to the class of *continuum percolation problems* [19]. The transport is determined by charge carriers with energies above the percolation level E_p, which is defined as the minimal energy that allows a transport path via connected regions with E_m not exceeding E_p.

Let $p(E)$ denote the volume fraction of regions where the mobility edge E_m is below E,

$$p(E) = \int_{-\infty}^{E} G(E_m)\, dE_m \ . \tag{16}$$

The quantity

$$\vartheta_c = p(E_p) \tag{17}$$

plays the role of the dimensionless percolation threshold determined as the minimal volume fraction of the conducting material that enables electrical connection throughout the infinitely large sample. Numerical studies for Gaussian energy distributions with various spatial correlation properties yield the value $\vartheta_c = 0.17 \pm 0.01$ for the three-dimensional continuum percolation problem [19]. Using the value $\vartheta_c = 0.17$ in Eq. (17), one obtains the value of the percolation level E_p

$$E_p = -0.95\,\delta \ . \tag{18}$$

It remains to determine the macroscopic conductivity σ from the regional conductivities $\sigma_{\text{region}}(E_m)$.

According to the percolation approach, only electrons with energies E above the threshold E_p determine the macroscopic conductivity. There are two options for such electrons: $E_m < E_p < E$ (mobile electrons in the "valleys") and $E_p < E_m < E$ (mobile electrons in the "mountain regions"). One might assume that it would be sufficient to take into account only regions with $E_m \leqslant E_p$ in order to determine the conductivity of the system. However, one should take into account that the transport path at the energy level $E = E_p$ is negligibly thin [19,27,30]. Therefore, electrons have to climb to the energies larger than E_p and, concomitantly, to explore the regions with $E_m > E_p$. In other words, each conducting path goes not only through places with $E_m < E_p$ ("valleys") but also through short regions with $E_m > E_p$ ("mountain passes"). The latter regions dominate the resistivity of the system, because they are the most resistive parts of the conduction path and they are connected in series with the less resistive "valleys." The higher the band edge E_m, the lower the local electron concentration, and consequently the larger the local resistivity. For this reason, when calculating the conductivity or mobility, only places with band edge E_m above the threshold E_p are decisive for charge transport. These places possess the highest resistivity among those, which belong to the percolation path. One can find more details to this issue in the review papers [27,30]. The simplest recipe to calculate σ on the basis of percolation theory is to average the regional conductivities over the regions where $E_m > E_p$,

$$\sigma = \frac{1}{1-\vartheta_c} \int_{E_p}^{+\infty} \sigma_{\text{region}}(E_m)\, G(E_m)\, dE_m \ , \tag{19}$$

where $G(E_m)$ is the Gaussian distribution of the local mobility edges E_m. The mobility $\mu = \sigma/en$ that corresponds to Eq. (19) can be expressed as

$$\mu = \mu_0 \frac{n_{\text{mob}}}{n} \ , \tag{20}$$

where n_{mob} is the average concentration of *mobile* electrons in the regions with $E_m > E_p$, and n is the total electron concentration. It is easy to recognize that Eq. (19) gives the correct value of the conductivity $\sigma = e\mu_0 n$ in the absence of disorder, $\delta = 0$.

Equation (19) also gives the correct value in the opposite limit of very pronounced disorder, $kT \ll \delta$, for a nondegenerate occupation of states above E_p, when the regional conductivities $\sigma_{\text{region}}(E_m)$ have an exponentially broad distribution of values. In this case, the Fermi function can be approximated as $f(E) = \exp[(E_f - E)/kT]$ and Eq. (14) yields the exponential dependence

$$\sigma_{\text{region}}(E) = e\mu_0 N_c \exp\left(\frac{E_f - E}{kT}\right) , \tag{21}$$

where N_c is the effective density of states in the conduction band,

$$N_c = \int_0^{+\infty} g(E) \exp(-E/kT)\, dE \ . \tag{22}$$

Inserting Eq. (21) into Eq. (19) gives the asymptotic expression for the carrier mobility

$$\mu = \frac{\sigma}{en} = \frac{\mu_0 N_c}{n(1-\vartheta_c)} \int_{E_p}^{+\infty} \exp\left(\frac{E_f - E}{kT}\right) G(E)\, dE \ . \tag{23}$$

At low temperatures, $kT \ll \delta$, the main contribution to the integral comes from the vicinity of the percolation level E_p. Therefore, one can approximately replace $G(E)$ by $G(E_p)$ and take the constant factor $G(E_p)$ out of the integral. The remaining integral is elementary and the carrier mobility given by Eq. (20) assumes its asymptotic form

$$\mu \approx \mu_0 \frac{N_c}{n} \frac{G(E_p)\, kT}{1-\vartheta_c} \exp\left(\frac{E_f - E_p}{kT}\right) . \tag{24}$$

The exponential term in Eq. (24) shows that the charge transport is dominated by thermal activation of electrons to the percolation level E_p, as schematically depicted in Fig. 2. More sophisticated considerations [19,28] lead to a marginal correction of the pre-exponential factor in this equation. In fact, the pre-exponential factor should contain $(kT)^{\nu}$ instead of kT where $\nu \simeq 0.88$ is the critical exponent for the correlation length of the percolation cluster [31–33]. Below, we will use Eq. (24) and ignore this marginal correction.

B. Averaging procedure by Adler *et al.*

In several theoretical studies of charge transport in AOS, the percolation approach suggested by Adler *et al.* [9] has been invoked [4,34]. Adler *et al.* [9] considered a system with a Gaussian distribution of the regional band edges as given by Eq. (8). They suggested that the global conductivity σ can be obtained as

$$\sigma_{\rm A} = \frac{1}{kT}\int_{E_p}^{+\infty} \sigma(E) f(E)[1-f(E)]\,dE\ . \tag{25}$$

Here $\sigma(E)$ is the contribution to the conductivity of carriers with energy E,

$$\sigma(E) = \tilde{B}[p(E)-\vartheta_c]^2, \tag{26}$$

where $\tilde{B}$ is some unspecified constant.

For a comparison with our approach in Sec. III A, we analyze the conductivity $\sigma_{\rm A}$ from Eq. (25) when the Fermi level is far below the percolation level, $E_f < E_p$ and $kT \ll E_p - E_f$. Then, we can use the Boltzmann approximation $f(E) \approx \exp[(E_f - E)/kT]$ and $1 - f(E) \approx 1$ for the Fermi functions in Eqs. (25) and (26) in the nondegenerate case, leading to

$$\sigma_{\rm A} = \frac{\tilde{B}}{kT}\int_{E_p}^{+\infty} \exp\left(\frac{E_f - E}{kT}\right)[p(E)-\vartheta_c]^2\,dE\ . \tag{27}$$

At low temperatures, $kT \ll \delta$, the major contribution to this integral comes from the region $E \approx E_p$, providing $G(E) \approx G(E_p)$. Using Eqs. (16) and (17), the factor $[p(E) - \vartheta_c]$ can be simplified to

$$p(E) - \vartheta_c = \int_{E_p}^{E} G(E')\,dE' \approx (E - E_p)G(E_p)\ . \tag{28}$$

Concomitantly, Eq. (27) simplifies to

$$\sigma_{\rm A} \approx \frac{\tilde{B}}{kT}[G(E_p)]^2\int_{E_p}^{+\infty} \exp\left(\frac{E_f - E}{kT}\right)(E - E_p)^2\,dE\ . \tag{29}$$

The integral is elementary. Using its value in Eq. (29), we obtain the asymptotic expression for the mobility

$$\mu_{\rm A} \approx \frac{2\tilde{B}[G(E_p)]^2(kT)^2}{en}\exp\left(\frac{E_f - E_p}{kT}\right). \tag{30}$$

A comparison of this expression with the result of percolation theory in Eq. (24) shows that the exponential term is correctly reproduced by Eq. (30). However, besides the unknown coefficient $\tilde{B}$, Eq. (30) displays an incorrect temperature dependence of the pre-exponential factor due to the assumption of a quadratic energy dependence of the regional conductivity above the threshold, see Eq. (26).

The (global) band-edge E_m in the random-barrier model, as described in Sec. I A, and the percolation threshold E_p are unrelated conceptually. However, the question remains: Is it possible to interpret the energy level E_m in the model sketched in Fig. 1 as the percolation level E_p in Fig. 2 so that the random-barrier model can be viewed as part of the random band-edge model for energies above the percolation level, $E > E_p$? Unfortunately, this is not the case. First, the random-barrier model in Fig. 1 cannot contain a recipe on how to calculate the percolation level E_p. Second, since E_m is a regional feature determined by the distribution (8), one cannot consider the value E in Eqs. (2) and (4) as if E_m were uniform for the whole system. Therefore, an approach based on replacing E_m in Fig. 1 by the percolation level E_p would not make sense.

In Sec. V, we will compare the predictions of the percolation theory expressed by Eq. (19) with experimental data obtained by several experimental groups on the dependences of the carrier mobility $\mu(n,T)$ on the carrier concentration n and temperature T in IGZO materials [2,4,8,29]. Before that we address in Sec. IV the relation between the results from percolation theory and those based on the effective-medium approximation (EMA).

IV. COMPARISON BETWEEN PERCOLATION THEORY AND EMA

The EMA and percolation theory are often considered complementary to each other in their ability to account for charge transport in disordered systems. Percolation theory is considered to be valid for strongly disordered systems [19], while in systems with a weak disorder the EMA is often applied [29]. In fact, percolation theory gives reliable results not only for the case of strong disorder, $kT \ll \delta$, but also for the opposite case of $\delta \to 0$, as discussed in Sec. III in the context of Eq. (19). Therefore, it is instructive to estimate the difference between the results of percolation theory and those of the EMA in the case of strong disorder.

In the EMA framework used by Fishchuk *et al.* [29] the conductivity σ was determined from its regional values $\sigma_{\rm region}(E_m)$ via the equation

$$\left\langle \frac{\sigma_{\rm region} - \sigma}{\sigma_{\rm region} + (d-1)\sigma} \right\rangle = 0\ , \tag{31}$$

where d is the spatial dimension, and the angular brackets mean the averaging over the density distribution function $G(E_m)$

$$\langle \mathcal{A} \rangle \equiv \int_{-\infty}^{+\infty} G(E_m)\mathcal{A}(E_m)\,dE_m\ . \tag{32}$$

To calculate the carrier mobility $\mu(n,T)$ in the framework of the EMA, one should calculate the Fermi level E_f from Eqs. (10)–(13) and then determine the dependence of the regional conductivity $\sigma_{\rm region}(E_m)$ on the regional mobility edge E_m, which then leads to the global conductivity σ via Eq. (31) and to the carrier mobility μ via Eq. (15).

Let us rewrite the averaging condition (31) in the following equivalent form in three dimensions, $d = 3$,

$$\left\langle \frac{\sigma_{\rm region}}{\sigma_{\rm region} + 2\sigma} \right\rangle = \frac{1}{3}\ . \tag{33}$$

In the limit of low temperature and low electron concentration, the dependence $\sigma_{\rm region}(E_m)$ of the regional conductivity on the regional conduction band edge E_m is very steep, i.e., for almost all values of E_m we have either $\sigma_{\rm region}(E_m) \gg 2\sigma$ or $\sigma_{\rm region}(E_m) \ll 2\sigma$. In the first case, the expression inside the angular brackets in Eq. (33) is close to unity, in the second

case, it is close to zero. Therefore,

$$\frac{\sigma_{\rm region}(E_m)}{\sigma_{\rm region}(E_m)+2\sigma} \approx \begin{cases} 1 & \text{if } E_m < E^* \,, \\ 0 & \text{if } E_m > E^* \,, \end{cases} \tag{34}$$

where E^* is the value of E_m that separates these two limits,

$$\sigma_{\rm region}(E^*) = 2\sigma \ . \tag{35}$$

Inserting Eq. (34) into Eq. (33), and using the rule of averaging (32), one can evaluate Eq. (33) as

$$\int_{-\infty}^{E^*} G(E_m)\, dE_m = \frac{1}{3} \ . \tag{36}$$

This equation defines the energy E^*.

In the case of Gaussian distribution function $G(E_m)$, Eq. (8), the solution is

$$E^* \approx -0.43\,\delta \ . \tag{37}$$

With this value for E^*, one can find the macroscopic conductivity σ from Eq. (35), where $\sigma_{\rm region}(E^*)$ is to be calculated from Eq. (14). Inserting Eq. (21) into Eq. (35) provides the following asymptotic expression for the mobility $\mu = \sigma/en$,

$$\mu \approx \mu_0 \frac{N_c}{2n} \exp\left(\frac{E_f - E^*}{kT}\right) . \tag{38}$$

The expression (38) is valid when $E_f < E^*$, $kT \ll E^* - E_f$ and $kT \ll \delta$.

According to Eq. (38) one can interpret the transport in the low-temperature and low-concentration case as thermal activation of electrons to the energy level E^*. This result is to be compared with that of the percolation theory given by Eq. (24). Even if we ignore the differences in the pre-exponential factors we can conclude that the results given by Eqs. (38) and (24) differ by an exponential factor $\propto\exp(-0.52\,\delta/kT)$, which is essential for strong disorder, $kT \ll \delta$.

However, this result is specific to the present case and does not imply that the EMA framework always leads to an exponentially large error in the case of strong disorder. As has been shown in several studies [35,36], one can achieve a better description of the conductivity within the EMA framework by replacing the spatial dimension $d = 3$ with the inverse of the percolation threshold $1/\vartheta_c \approx 6$. However, conceptual improvements of the EMA are beyond the scope of our present study. Instead, in next Sec. V we turn to a comparison between the results of percolation theory from Sec. III and experimental data.

V. COMPARISON WITH EXPERIMENTAL DATA

In this section, we show that the percolation approach developed in Sec. III and applied to the random band-edge model presented in Sec. II is able to reproduce experimental data on charge transport in InGaZnO materials. The main theoretical result to be compared with experimental data is Eq. (19) for the conductivity $\sigma(n, T)$, as discussed in Sec. III. The regional conductivity $\sigma_{\rm region}(E_m)$ in this equation is given by Eq. (14), where the regional density of states $g(E - E_m)$ is taken in the form of Eq. (10) with $g_c = 10^{21}$ cm^{-3} eV$^{-3/2}$.

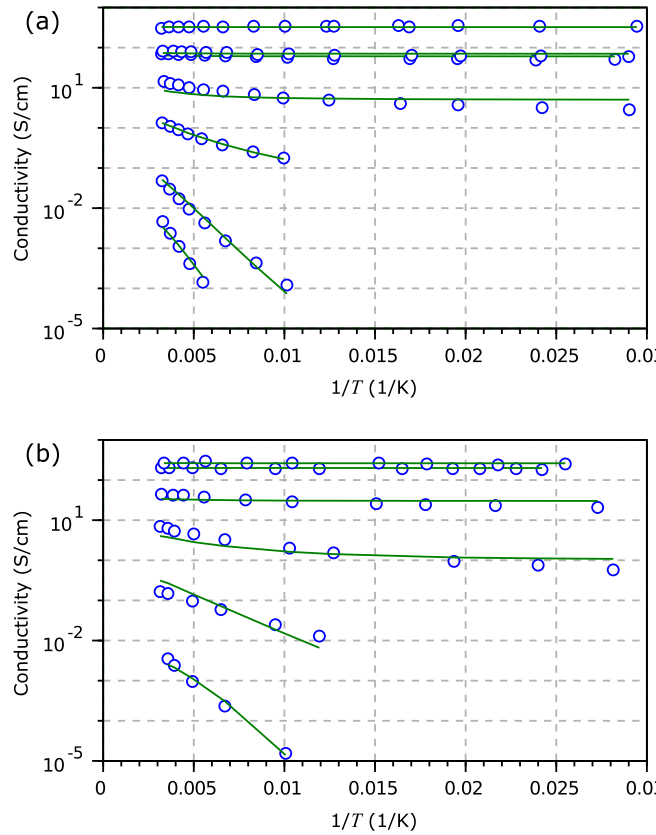

FIG. 3. Temperature dependence of the conductivity $\sigma(T)$ in c-IGZO (a) and a-IGZO (b) samples with different carrier concentration n. Circles: experimental data [4]. Solid lines: fit to Eq. (19). The values of fitting parameters are specified in the text.

Following Ref. [29], we take into account the distribution $G(E_m)$ of the regional positions of the band edge E_m in the form of Eq. (8) and neglect for simplicity the presence of localized states with energies below E_m by setting $N_m = 0$. We address experimental data for the temperature dependencies of conductivity $\sigma(T)$ and mobility $\mu(T)$ at different concentrations of charge carriers n. The carrier concentration is changed experimentally either by varying the doping level [4] or by varying the gate voltage in the field-effect transistors [8,18,29].

In their pioneering works [2,4], Kamiya *et al.* investigated two series of n-type IGZO films: crystalline (c-IGZO) and amorphous (a-IGZO). Samples of c-IGZO are crystalline materials but they contain inherent disorder due to the statistical distribution of Ga and Zn ions. Therefore, such materials are to be considered as disordered materials with respect to charge transport [4]. In each series of the samples, the conductivity $\sigma(T)$ was measured varying the carrier concentrations n between $n < 10^{16}$ cm^{-3} and $n \sim 10^{20}$ cm^{-3} [4].

Experimental data on the temperature dependencies of the conductivity $\sigma(T)$ are shown by circles in Fig. 3(a) for c-IGZO and in Fig. 3(b) for a-IGZO. These data are copied from Fig. 1(b), and Fig. 1(d) of Ref. [4], respectively. Theoretical results given by Eq. (19) are shown in Fig. 3 by solid lines. These results are obtained by adjusting the band-edge disorder parameter δ in Eq. (8) and the conduction-band mobility μ_0, keeping these parameters fixed for *each group*

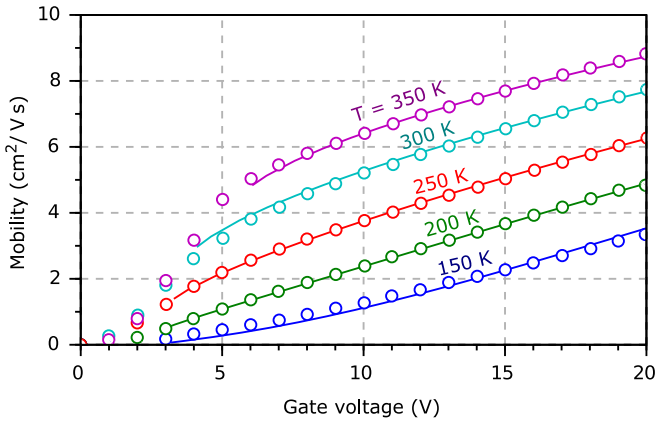

FIG. 4. Dependence of the carrier mobility μ on the gate voltage V_g at different temperatures. Circles: experimental data [8]. Solid lines: fit $\mu(n,T)=\sigma(n,T)/(en)$, where $\sigma(n,T)$ is given by Eq. (19). The values of fitting parameters are specified in the text.

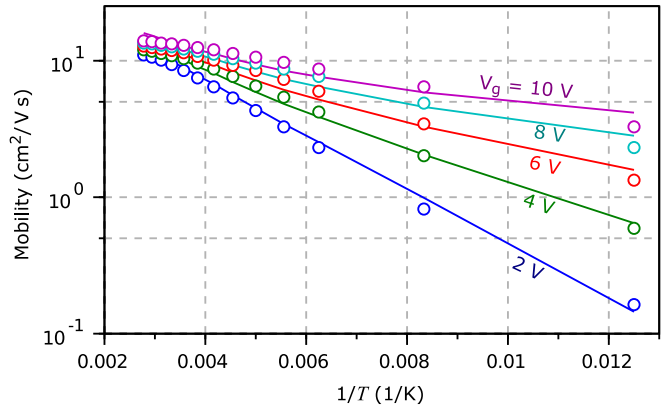

FIG. 5. Dependence of the carrier mobility $\mu(V_g,T)$ on temperature at different gate voltages V_g. Circles: experimental data [29]. Solid lines: fit of $\mu(n,T)=\sigma(n,T)/(en)$, where $\sigma(n,T)$ is given by Eq. (19). The values of fitting parameters are specified in the text.

of samples. Since the values of the carrier concentration n in different samples were not exactly specified [4], we use n as an adjustable parameter. Values for n in the range between $n=10^{15}$ cm^{-3} and $n=6\times10^{19}$ cm^{-3} give the best fits, in good agreement with experimental estimates [4]. The parameters δ, μ_0, and n are considered as independent of temperature. The values of δ and μ_0 that provide the best fit to the experimental data are $\delta=0.057$ eV, $\mu_0=39$ cm^2/Vs for c-IGZO, and $\delta=0.036$ eV, $\mu_0=47$ cm^2/Vs for a-IGZO. It is not obvious why amorphous samples should possess a slightly higher carrier mobility as compared to the crystalline ones. One should, however, take into account that c-IGZO and a-IGZO films were created by different technological techniques: a reactive solid-phase epitaxy method for c-IGZO and pulsed laser deposition for a-IGZO. One can expect different factors resulting in the energy disorder and electron scattering (nonstoichiometry, dangling bonds, etc.) due to different technological techniques.

Another set of experimental data to be compared with theoretical predictions is related to the carrier mobility $\mu(n,T)$ measured in thin-film transistors with IGZO channels [8,29]. In Fig. 4, experimental data for the dependencies of μ on the gate voltage V_g at different temperatures are reproduced from Ref. [8] as depicted by circles. Solid lines are the theoretical results for $\mu(n,T)=\sigma(n,T)/(en)$, where $\sigma(n,T)$ is obtained from Eq. (19). The carrier concentration n is assumed linearly dependent on the gate voltage V_g,

$$n=\lambda[V_g-V^*(T)]\,, \tag{39}$$

where the proportionality constant λ serves as a fitting parameter. It depends on the relative capacitance between the gate and the channel and on the thickness of the electron accumulation layer. The value $\lambda=9.11\times10^{16}$ cm^{-3} V^{-1} gives the best fit. Following Ref. [8], the experimental gate voltage is counted from its threshold value. The flat-band voltage V^* is also treated as an adjustable parameter. Following Ref. [29], V^* is considered temperature dependent. This dependence could be caused by the temperature dependence of the density of surface charges at the interface IGZO/SiO$_2$. The values $V^*=2.69$ V, 2.32 V, 2.79 V, 3.61 V, 5.57 V are used for $T=150$ K, 200 K, 250 K, 300 K, 350 K, respectively. The best fits to the experimental data in Fig. 4 are achieved by choosing the band-edge disorder parameter $\delta=0.063$ eV in Eq. (8) and the conduction-band mobility $\mu_0=30$ cm^2/Vs. The lower bound on the curves in Fig. 4 is 0.5 Volts above V^*, so it is different at different temperatures. A noticeable conduction below V^* at $T=250$ K and at higher T could be due to electrons in the bulk of IGZO films.

Experimental data on the carrier mobility in a-IGZO thin-film transistors, analogous to those in Fig. 4, were obtained by Fishchuk *et al.* [29] who converted the data into $\mu(T)$ at different gate voltages V_g. The data are shown by circles in Fig. 5. Solid lines are fits to Eq. (19). The temperature dependence of V^* in Eq. (39) is taken from Ref. [29], $V^*(T)=-1.61$ V $+109$ V$/(T/\mathrm{K})$. The value $\lambda=1.32\times10^{17}$ cm^{-3} V^{-1} gives the best fit. The best agreement with experimental data in Fig. 5 is achieved by choosing the band-edge disorder parameter $\delta=0.05$ eV in Eq. (8) and the conduction-band mobility $\mu_0=36$ cm^2/(Vs). These values are close to the values $\delta=0.04$ eV and $\mu_0=22$ cm^2/(Vs) obtained by Fishchuk *et al.* [29] from a comparison of their experimental data and their theory based on the EMA. This evidences that there is not much difference between the results of the percolation theory and those of the EMA for the range of parameters δ, kT, n, and μ_0 relevant to the experimental situation studied in Ref. [29].

For a fairly small range of parameters, 36 meV $<\delta<$ 63 meV and 30 cm^2/(Vs) $<\mu_0<$ 47 cm^2/(Vs) for the band-edge disorder parameter δ in Eq. (8) and the conduction-band mobility μ_0, percolation theory reliably reproduces different sets of experimental data in IGZO materials over a broad range of temperatures and charge carrier densities.

VI. CONCLUSIONS

Theoretical approach based on the percolation theory is developed to describe charge transport in amorphous oxide semiconductors in the framework of the random band-edge model that takes into account the effect of disorder on the

regional position of the band edge E_m. For the case of a Gaussian distribution for E_m, the superiority of the percolation approach is proven in comparison with previously used averaging schemes. Our percolation approach reproduces experimental data on charge transport in IGZO materials obtained by several groups. The comparison between theoretical results and experimental data reveals the energy scale of disorder in such materials.

ACKNOWLEDGMENTS

The authors are indebted to Prof. A. Kadashchuk and to Prof. H. Hosono for bringing their attention to the problem of charge transport in AOS. Financial support of the Deutsche Forschungsgemeinschaft (GRK 1782) is gratefully acknowledged. A.V.N. and A.V.D. acknowledge financial support by the Siberian branch of the Russian Academy of Sciences (integration Project No. 7).

[1] K. Nomura, H. Ohta, A. Takagi, T. Kamiya, M. Hirano, and H. Hosono, Nature (London) **432**, 488 (2004).

[2] T. Kamiya, K. Nomura, and H. Hosono, J. Disp. Technol. **5**, 462 (2009).

[3] A. Takagi, K. Nomura, H. Ohta, H. Yanagi, T. Kamiya, M. Hirano, and H. Hosono, Thin Solid Films **486**, 38 (2005).

[4] T. Kamiya, K. Nomura, and H. Hosono, Appl. Phys. Lett. **96**, 122103 (2010).

[5] M. Kimura, T. Kamiya, T. Nakanishi, K. Nomura, and H. Hosono, Appl. Phys. Lett. **96**, 262105 (2010).

[6] R. H. Bube, *Electronic Properties of Crystalline Solids: An Introduction to Fundamentals* (Academic Press, New York, London, 1974).

[7] S. M. Sze, *Physics of Semiconductor Devices*, 2nd ed. (Wiley, New York, 1981).

[8] W. C. Germs, W. H. Adriaans, A. K. Tripathi, W. S. C. Roelofs, B. Cobb, R. A. J. Janssen, G. H. Gelinck, and M. Kemerink, Phys. Rev. B **86**, 155319 (2012).

[9] D. Adler, L. P. Flora, and S. D. Sentuna, Solid State Commun. **12**, 9 (1973).

[10] J.-H. Park, K. Jeon, S. Lee, S. Kim, S. Kim, I. Song, J. Park, Y. Park, C. J. Kim, D. M. Kim, and D. H. Kim, J. Electrochem. Soc. **157**, H272 (2010).

[11] S. Lee, S. Park, S. Kim, Y. Jeon, K. Jeon, J.-H. Park, J. Park, I. Song, C. J. Kim, Y. Park, D. M. Kim, and D. H. Kim, IEEE Electron Device Lett. **31**, 231 (2010).

[12] N. F. Mott and E. A. Davis, *Electronic Processes in Non-Crystalline Materials*, 2nd ed. (Clarendon Press, Oxford, 1979).

[13] H. Overhof and P. Thomas, *Electronic Transport in Hydrogenated Amorphous Semiconductors* (Springer, Heidelberg, 1989).

[14] R. A. Street, *Hydrogenated Amorphous Silicon*, Cambridge Solid State Science Series (Cambridge University Press, New York, 1991).

[15] S. Baranovski (ed.) *Charge Transport in Disordered Solids with Applications in Electronics* (John Wiley & Sons, Ltd, Chichester, 2006).

[16] O. Semeniuk, G. Juska, J. O. Oelerich, K. Jandieri, S. D. Baranovskii, and A. Reznik, J. Phys. D **50**, 035103 (2017).

[17] S. Lee, K. Ghaffarzadeh, A. Nathan, J. Robertson, S. Jeon, C. Kim, I.-H. Song, and U.-I. Chung, Appl. Phys. Lett. **98**, 203508 (2011).

[18] S. Lee and A. Nathan, Appl. Phys. Lett. **101**, 113502 (2012).

[19] B. I. Shklovskii and A. L. Efros, *Electronic Properties of Doped Semiconductors* (Springer, Berlin, 1984).

[20] M. Grünewald and P. Thomas, Phys. Status Solidi B **94**, 125 (1979).

[21] D. Monroe, Phys. Rev. Lett. **54**, 146 (1985).

[22] S. D. Baranovskii, P. Thomas, and G. J. Adriaenssens, J. Non-Cryst. Solids **190**, 283 (1995).

[23] S. D. Baranovskii, T. Faber, F. Hensel, and P. Thomas, J. Phys.: Condens. Matter **9**, 2699 (1997).

[24] S. D. Baranovskii, H. Cordes, F. Hensel, and G. Leising, Phys. Rev. B **62**, 7934 (2000).

[25] S. D. Baranovskii, I. P. Zvyagin, H. Cordes, S. Yamasaki, and P. Thomas, Phys. Status Solidi B **230**, 281 (2002).

[26] S. D. Baranovskii, Phys. Status Solidi B **251**, 487 (2014).

[27] A. V. Nenashev, J. O. Oelerich, and S. D. Baranovskii, J. Phys.: Condens. Matter **27**, 093201 (2015).

[28] A. V. Nenashev, F. Jansson, J. O. Oelerich, D. Huemmer, A. V. Dvurechenskii, F. Gebhard, and S. D. Baranovskii, Phys. Rev. B **87**, 235204 (2013).

[29] I. I. Fishchuk, A. Kadashchuk, A. Bhoolokam, A. de Jamblinne de Meux, G. Pourtois, M. M. Gavrilyuk, A. Köhler, H. Bässler, P. Heremans, and J. Genoe, Phys. Rev. B **93**, 195204 (2016).

[30] J. C. Dyre and T. B. Schrøder, Rev. Mod. Phys. **72**, 873 (2000).

[31] J. Wang, Z. Zhou, W. Zhang, T. M. Garoni, and Y. Deng, Phys. Rev. E **87**, 052107 (2013).

[32] H. Hu, H. W. J. Blöte, R. M. Ziff, and Y. Deng, Phys. Rev. E **90**, 042106 (2014).

[33] Z. Koza and J. Poła, J. Stat. Mech.: Theory Exp. (2016) 103206.

[34] W. C. Germs, J. J. M. van der Holst, S. L. M. van Mensfoort, P. A. Bobbert, and R. Coehoorn, Phys. Rev. B **84**, 165210 (2011).

[35] M. Nakamura, Phys. Rev. B **29**, 3691 (1984).

[36] Y. Chen and C. A. Schuh, Acta Mater. **54**, 4709 (2006).